

# Detection and Distinction of DNT and TNT with a Fluorescent Conjugated Polymer Using the Microwave Conductivity Technique

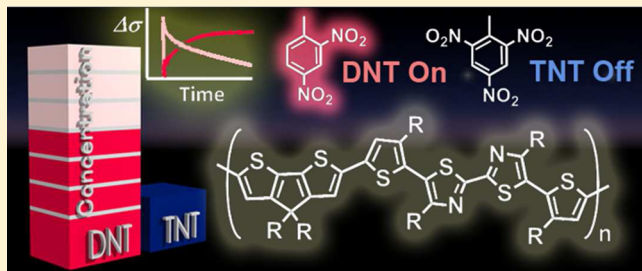
Bijitha Balan,<sup>†</sup> Chakkooth Vijayakumar,<sup>†</sup> Masashi Tsuji,<sup>†</sup> Akinori Saeki,<sup>\*,†,‡</sup> and Shu Seki<sup>\*,†</sup>

<sup>†</sup>Department of Applied Chemistry, Graduate School of Engineering, Osaka University, 2-1 Yamadaoka, Suita, Osaka 565-0871, Japan

<sup>‡</sup>PRESTO, Japan Science and Technology Agency (JST), 4-1-8 Honcho Kawaguchi, Saitama 332-0012, Japan

## S Supporting Information

**ABSTRACT:** We report the detection and distinction of dinitrotoluene (DNT) and trinitrotoluene (TNT) by the microwave conductivity technique using a cyclopentadithiophene–bithiazole-based polymer (CPDT-BT) as sensor. Although the conventional fluorescence quenching experiments showed just “turn OFF” of the polymer fluorescence for both DNT and TNT, time-resolved microwave conductivity (TRMC) revealed that the photoconductivity of the polymer, which is “turned OFF” in the pristine state became “ON” in the presence of DNT but remained “OFF” with TNT, allowing easy distinction between them. Moreover, the decay rate of the transient kinetics was found to be sensitive to the DNT concentration, implementing a unique method for the determination of unknown DNT concentration. The observations are discussed in viewpoint of charge separation (CS) and formation of charge transfer (CT) complex by considering deeper LUMO of TNT than DNT calculated from the DFT method. This study brings out a novel technique of speedy detection and distinction of environmentally important analytes, an alternative to the fluorescence quenching.



## 1. INTRODUCTION

Explosives detection has received a significant attention during the recent years not only for homeland security and forensic analysis but also for the environmental assessment.<sup>1,2</sup> Several methods and technologies aimed at detecting the explosives in vapor or bulk state are available at present.<sup>3–9</sup> In this context, organic conjugated polymers are particularly important due to cost efficiency, sensitivity, portability, and faster signal analysis.<sup>10,11</sup> Most of the reported conjugated polymers for explosives detection are based on pentiptycene, *p*-phenyleneethynlenes, *p*-phenylenevinylenes, carbazoles, thiophenes, silafluorenes, metalloles, triazoles, etc.<sup>12–22</sup> A vast majority of the detection methods with conjugated polymers utilize the fluorescence “turn OFF” phenomenon due to the photo-induced electron transfer in the presence of analyte. As the detection mechanism is mainly based on the fluorescence quenching processes, these sensors suffer from the intrinsic selectivity problem in a complex environment. In most cases, there is no clear discrimination between the different analytes which consists of nitro functional groups, although the sensory response could be slightly different toward different analytes. For instance, it is difficult to distinguish between dinitrotoluene (DNT) and trinitrotoluene (TNT) since both of them are very good electron acceptors and hence quench the polymer fluorescence efficiently. However, selectivity is really important when it comes to practical applications, and it is important to develop novel materials and methods to overcome such issues.

Herein we report the detection of DNT and TNT with a fluorescent conjugated polymer and introduce a novel method

for their distinction using the flash-photolysis time-resolved microwave conductivity (FP-TRMC) technique. FP-TRMC is an electrodeless conductivity measurement technique which is highly useful for the evaluation of charge carrier generation and mobility in organic materials on photoexcitation. The charge carrier generation is known to be sensitive to the electronic energy levels of the donor and acceptor (analyte) systems. We anticipated that difference in HOMO–LUMO levels of DNT and TNT might result in different charge carrier generation properties when complexed with a suitable donor and hence allow easy distinction between them.

## 2. EXPERIMENTAL SECTION

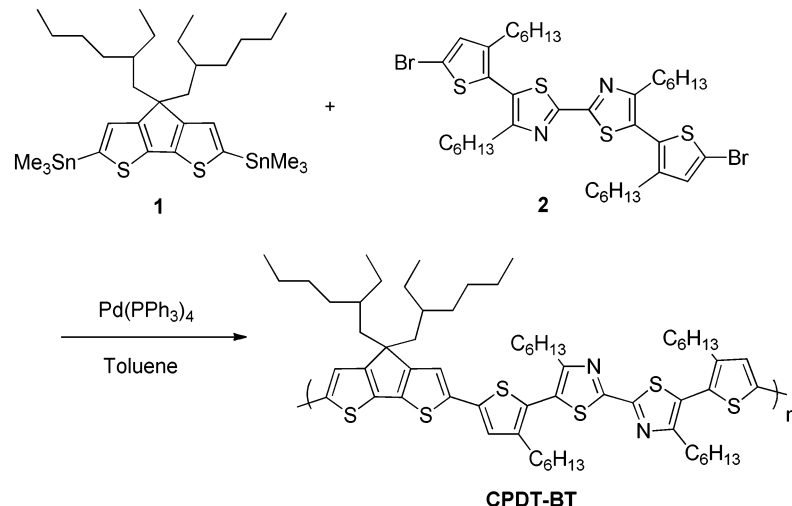
**2.1. Materials.** All chemicals were purchased from Aldrich, Kanto Chemicals, TCI, or Wako and used as received. Air- and water-sensitive synthetic steps were performed in an argon atmosphere using standard Schlenk techniques.

**2.2. Measurements.** <sup>1</sup>H and <sup>13</sup>C NMR spectra were recorded on a 600 MHz Varian UNITY Inova spectrometer. All the chemical shifts were referenced to (CH<sub>3</sub>)<sub>4</sub>Si (TMS; δ = 0 ppm) for <sup>1</sup>H or residual CHCl<sub>3</sub> (δ = 77 ppm) for <sup>13</sup>C. The molecular weights of the polymer were measured by gel permeation chromatography (GPC, Hitachi, L-2130, L-2350, L-2455) in tetrahydrofuran solution calibrated against polystyrene standards. Electronic absorption spectra were recorded on a

Received: May 17, 2012

Revised: July 23, 2012

Published: August 3, 2012

**Scheme 1.** Synthetic Procedure for Polymer CPDT-BT

JASCO V-570 spectrophotometer, and the emission spectra of the solution state were recorded on a Hitachi F-2700 spectrophotometer. Fluorescence quenching experiments were carried out by microtitration in solution in a quartz cuvette. Emission spectra in the film state were recorded on an II-equipped streak camera C7700 of Hamamatsu Photonics Inc. using a third harmonic generation (355 nm) from a nanosecond Nd:YAG laser of Spectra-Physics Inc. model INDY as an excitation wavelength. The fluorescence quenching of the thin films were measured by spin-coating chlorobenzene solutions containing 0.7 wt % of CPDT-BT and different known concentrations of analytes under rotation speed of 1000 rpm for 30 s. The film thickness was measured by a stylus surface profiler (ULVAC, Dektak 150) and was about 40 nm. Fluorescence quenching studies in film state by exposing to the explosives vapors (DNT and TNT) were done according to literature procedures.<sup>22</sup> Briefly, 1.5 g of powdered DNT or TNT was placed in a 50 mL glass vial. Some cotton was placed over the powdered explosives to avoid direct contact with the film. The sealed glass vial was kept overnight to get constant, saturated vapor pressure inside. The fluorescence spectra of the films were measured immediately after exposing to the explosives vapors for a specific time duration. Optical properties were measured in solution state and film state by using quartz cells (path length = 1 cm) and quartz plates, respectively.

**Flash-Photolysis Time-Resolved Microwave Conductivity.** Transient conductivity was measured by flash-photolysis time-resolved microwave conductivity (FP-TRMC). A resonant cavity was used to obtain a high degree of sensitivity in the measurement of conductivity. The resonant frequency and the microwave power were set at ~9.1 GHz and 3 mW, respectively, so that the electric field of the microwave was sufficiently small not to disturb the motion of charge carriers. The value of conductivity is converted to the product of the quantum yield ( $\phi$ ) and the sum of charge carrier mobilities ( $\sum \mu$ ) by the equation

$$\phi \sum \mu = \frac{1}{eAI_0F_{\text{light}}} \frac{\Delta P_r}{P_r} \quad (1)$$

where  $e$ ,  $A$ ,  $I_0$ ,  $F_{\text{light}}$ ,  $\Delta P_r$ , and  $P_r$  are the unit charge of a single electron, a sensitivity factor [ $(\text{S}/\text{m})^{-1}$ ], incident photon density of excitation laser ( $\text{photons}/\text{m}^2$ ), a correction (or filling) factor ( $/\text{m}$ ), change of reflected microwave power, and power of

reflected microwave, respectively. The change of conductivity is equivalent with  $\Delta P_r/(AP_r)$ . Third harmonic generation (THG, 355 nm) of a Nd:YAG laser (Spectra-Physics Inc., INDI, 5–8 ns pulse duration) was used as an excitation source. The intensity of laser ( $I_0$ ) was changed by gradient neutral density filters. The incident photon density used in the present study was  $4.6 \times 10^{15} \text{ photons cm}^{-2}$ . The sample was set at the highest electric field in a resonant cavity. The experiments were carried out at room temperature.

**2.3. Synthesis.** Syntheses of monomers **1** and **2** were reported elsewhere,<sup>23,24</sup> and polymer CPDT-BT was synthesized according to Scheme 1.

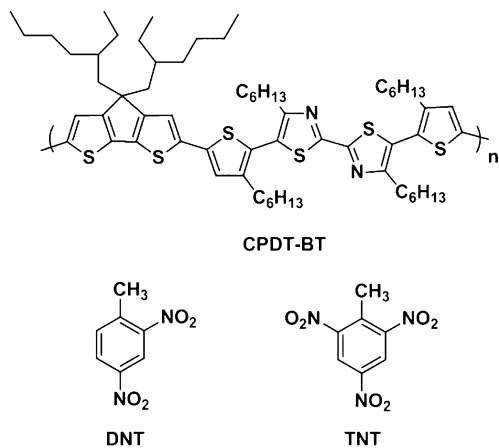
**Synthesis of CPDT-BT.** Monomer **1** (131 mg, 0.179 mmol, 1 equiv) and monomer **2** (148 mg, 0.179 mmol, 1 equiv) were weighed to a two-necked round-bottomed flask. Dry toluene (7 mL) was added to the reaction mixture. Air was removed from the flask and filled by nitrogen by using the freeze–thaw–pump method three times. Pd( $\text{PPh}_3$ )<sub>4</sub> (19 mg, 0.0179 mmol, 0.1 equiv) was added under N<sub>2</sub> counterflow, and the reaction mixture was refluxed at 100 °C for 3 days. After 3 days bromothiophene (1.5  $\mu\text{L}$ , 0.0179 mmol, 0.1 equiv) was added to the reaction mixture, 10 h later tributyl(thiophen-2-yl)stannane (6 mg, 0.0179 mmol, 0.1 equiv) was added, and the reaction refluxed overnight to complete the end-capping reaction. The resultant polymer solution was cooled down to room temperature and diluted by adding toluene (20 mL), and the polymer was precipitated by slowly adding the mixture into methanol (250 mL). The precipitates were collected by filtration and washed with methanol. The solid was then dissolved in chloroform and passed through a silica column using chloroform as an eluent. The combined polymer solution was passed through Celite, concentrated, and reprecipitated in methanol. Then it was purified by Soxhlet extraction using acetone and ethyl acetate, refluxing 1 day with each solvent. After that, it was extracted in chloroform, concentrated and dried. GPC:  $M_w = 31\,000 \text{ g mol}^{-1}$ ;  $M_n = 16\,800 \text{ g mol}^{-1}$ ;  $M_w/M_n = 1.8$ . <sup>1</sup>H NMR (600 MHz, CDCl<sub>3</sub>):  $\delta$  7.0–7.10 (br, 4H), 2.45–2.65 (br, 4H), 2.70–2.80 (br, 4H), 1.65–1.99 (br, 8H), 0.61–1.50 (br, 70H).

### 3. RESULTS AND DISCUSSION

For effective detection of explosives via electron transfer reactions, we have synthesized a fluorescent conjugated donor

polymer CPDT-BT (Scheme 2), which consists of alternating cyclopentadithiophene (CPDT) donor unit and bithiazole

**Scheme 2. Structures of CPDT-BT, DNT, and TNT**



(BT) acceptor unit conjugated through a bridging thiophene moiety. CPDT-BT was synthesized by Stille polycondensation reaction and characterized using standard spectroscopic techniques. The molecular weight and polydispersity index were  $31\,000\text{ g mol}^{-1}$  and 1.8, respectively, with reference to polystyrene standards. It showed good solubility in common organic solvents like chloroform, chlorobenzene, toluene, THF, etc.

**3.1. Absorption Properties and DFT Calculations.** The steady-state photoabsorption and fluorescence emission of CPDT-BT in chlorobenzene solution and as thin film spin-coated from chlorobenzene solution (0.7 wt %) are shown in Figure 1A. The absorption maximum ( $\lambda_{\text{abs}}$ ) of the polymer was found at 466 nm in both the solution and film state, whereas

the emission maximum showed a marginal red-shift of 14 nm in the film state ( $\lambda_{\text{em}} = 583\text{ nm}$ ) than that in the solution ( $\lambda_{\text{em}} = 569\text{ nm}$ ). Most of the conjugated polymers exhibit significant bathochromic shift of absorption and emission maximum in film state due to planarization and interchain stacking effects.<sup>25–27</sup> So the absence of such shifts in this case indicates the absence of any planarization in the polymer backbone and also the lack of  $\pi-\pi$  stacking interactions between the polymer chains in the film state. This is in contrast to a similar polymer reported by Li et al.,<sup>23</sup> where the only difference is the absence of an alkyl chain on the thiophene unit, which exhibits  $\lambda_{\text{abs}}$  at 523 nm in solution and at 560 nm in the film state. The  $\lambda_{\text{abs}}$  of CPDT-BT is about 57 and 94 nm blue-shifted in solution and film states, respectively, when compared to the polymer reported by Lin et al. In order to have a better understanding of the polymer conformation, the energy-minimized structures were calculated using density-functional theory (DFT) at the B3LYP/6-31G(d,p) level. As shown in Figure 1B, the dihedral angles of BT-thiophene and CPDT-thiophene units in CPDT-BT were found to be  $55.14^\circ$  and  $14.7^\circ$ , respectively. The higher dihedral angle between the BT and thiophene units could be attributed to the steric interactions induced by alkyl chain present on the thiophene units. This nonplanar structure results in the blue-shift in the absorption maximum when compared to the polymer reported by Lin et al. The twisted geometry of the polymer backbone might also be preventing effective intrachain and interchain interactions in CPDT-BT in film state, leading to the absence of any significant red shift of absorption and emission maximum. The absence of stacking in CPDT-BT in the film state was further confirmed by X-ray diffraction (XRD) analysis (Figure S1). The XRD profile was broad and noisy without any significant peaks, indicating an amorphous nature of the polymer. However, this property is beneficial for sensing applications because the poor stacking of polymer chains provides more free volume for the analytes to

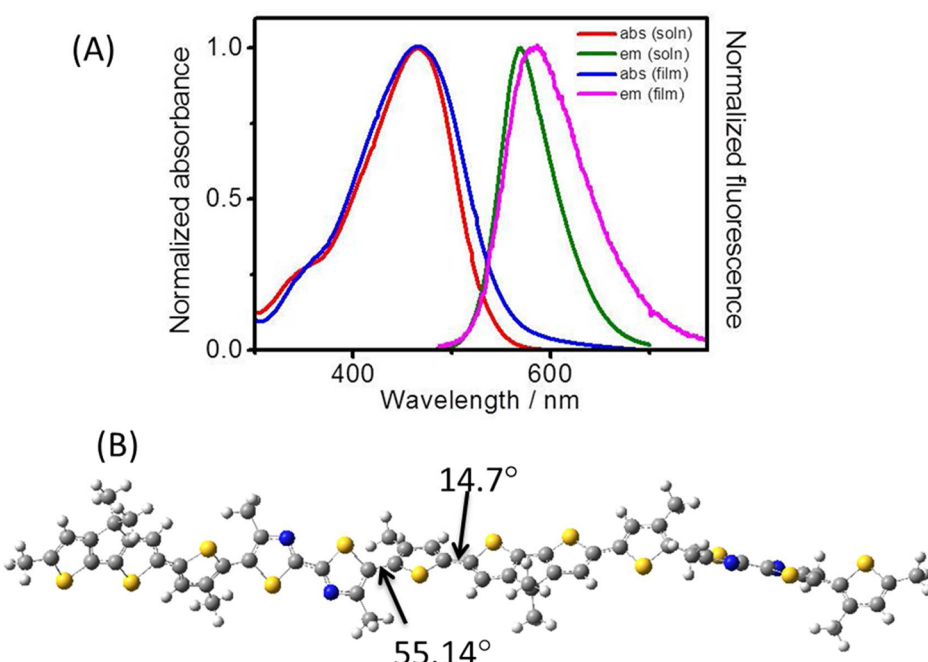


**Figure 1.** (A) Normalized absorption and emission spectra of CPDT-BT in chlorobenzene solution (concentration =  $1 \times 10^{-5}\text{ M}$ ,  $l = 1\text{ cm}$ ) and in thin film state (spin-coated from 0.7 wt % of CPDT-BT in chlorobenzene solution). (B) Optimized structure of two repeating units of CPDT-BT (alkyl chains were replaced by methyl for simplicity) obtained by the DFT calculation.

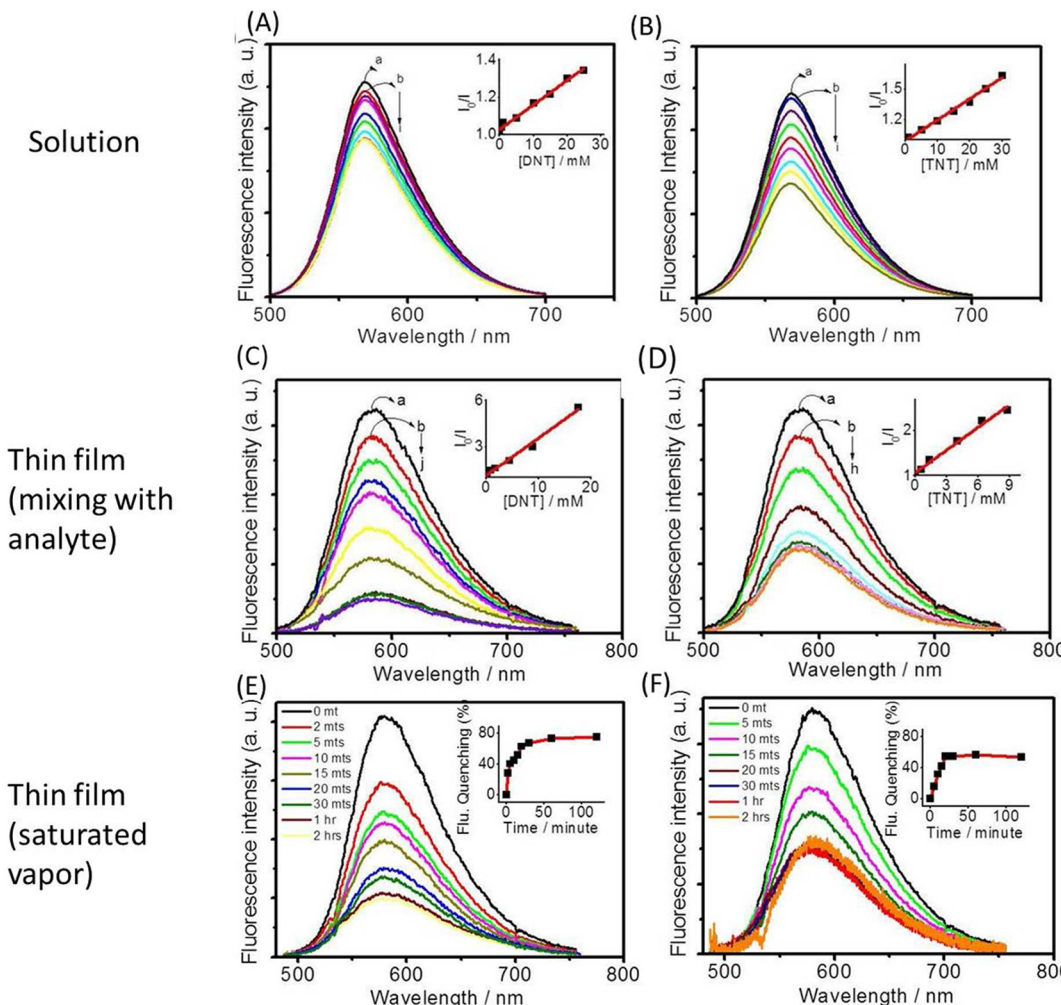


**Figure 2.** Fluorescence spectra of CPDT-BT in the (a) absence and (b–h/i/j) in the presence of different concentrations of analytes such as (A) DNT ( $5 \times 10^{-4}$ – $3 \times 10^{-2}$  M) in solution state, (B) TNT ( $1 \times 10^{-3}$ – $3.5 \times 10^{-2}$  M) in chlorobenzene solution (CPDT-BT concentration:  $4 \times 10^{-5}$  M,  $\lambda_{\text{ex}} = 455$  nm). (C) DNT ( $8.85 \times 10^{-5}$ – $2.6 \times 10^{-2}$  M) and (D) TNT ( $5.8 \times 10^{-4}$ – $1.9 \times 10^{-2}$  M) in film states (prepared from chlorobenzene solution of  $(7.1 \times 10^{-3}$  M) CPDT-BT in the presence of above-mentioned concentration of analyte,  $\lambda_{\text{ex}} = 355$  nm). Respective Stern–Volmer plots for the fluorescence quenching are shown in the inset of (A–D). Time-evolutional fluorescence quenching of CPDT-BT film upon exposure to saturated (E) DNT and (F) TNT vapors at room temperature ( $\lambda_{\text{ex}} = 355$  nm). Percentage of fluorescence quenching as a function of time is shown in the inset of (E) and (F).

interact with and also allows better diffusion of analytes into the film.

**3.2. Detection of DNT and TNT Using Fluorescence Quenching Measurements.** The explosives detection properties of the polymer was studied by fluorescence quenching measurements in the chlorobenzene solutions and in the thin films. The films were prepared by spin-coating 0.7 wt % of CPDT-BT in chlorobenzene ( $7.1 \times 10^{-3}$  M) containing varying amounts of DNT or TNT. The pristine films without analyte were also prepared and exposed to the saturated vapor of DNT or TNT, and the fluorescence spectra were sequentially measured. The fluorescence quantum yield of CPDT-BT was found to be 6% using fluorescein as the standard. Figures 2A and 2B show the progressive fluorescence quenching of CPDT-BT in presence of increasing concentrations of DNT and TNT in solution state. Similarly, the fluorescence quenching of the polymer in film state are shown in Figures 2C and 2D. The corresponding Stern–Volmer plots (fluorescence quenching vs quencher concentration) are shown in the insets of the respective figures. Figures 2E and 2F show

the time-dependent fluorescence quenching measurements of the polymer film on exposure to saturated vapors of DNT and TNT, respectively, at equilibrium pressure at room temperature. The corresponding percentage of fluorescence quenching as a function of time in the vapor state is shown in the inset. Fluorescence quenching of CPDT-BT in the presence of the analytes was comparatively slower in solution state than that of film state (bulk mixing as well as vapor exposure). This could be attributed to the enhanced interactions of the analytes with the polymer in film state. The Stern–Volmer plots exhibit a good linearity, giving Stern–Volmer constants ( $K_{\text{SV}}$ ) for the fluorescence quenching in the solution and film state from the slope of the respective plots. Quenching in the presence of TNT was faster with a  $K_{\text{SV}}$  of  $20.7 \text{ M}^{-1}$  in solution state compared to that of DNT ( $K_{\text{SV}} = 13.8 \text{ M}^{-1}$ ). In contrast to the solution state, the quenching efficiency was found to be more for DNT ( $K_{\text{SV}} = 244.6 \text{ M}^{-1}$ ) than that of TNT ( $166.5 \text{ M}^{-1}$ ) in the film state. In the case of TNT, quenching reaches saturation after a concentration of 9 mM (12.8 wt % in the mixture), whereas that of DNT reached at 18 mM (22.7 wt % in the

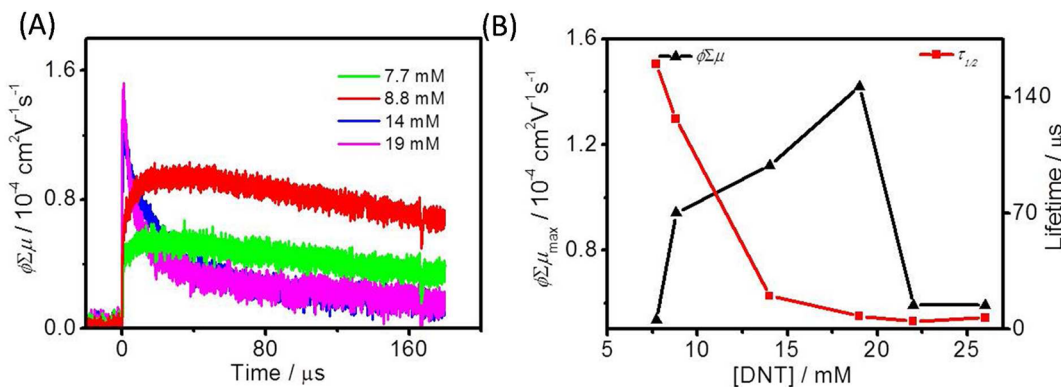


**Figure 3.** (A) FP-TRMC transients of CPDT-BT alone and in the presence of increasing concentrations of DNT. (B) Peak value of the transient photoconductivity ( $\phi \sum \mu_{\max}$ ) and lifetime ( $\tau_{1/2}$ ) as a function of concentration of DNT.

mixture). A more distinguishable difference was seen in the quenching of CPDT-BT on exposure to the saturated vapors of DNT and TNT. Much faster and efficient quenching was seen in the presence of DNT than that of TNT. This could be explained by considering the vapor pressures, which is about 18 times higher for DNT ( $144.36 \times 10^{-6}$  mmHg at  $25^\circ\text{C}$ ) than that of TNT ( $8.02 \times 10^{-6}$  mmHg at  $25^\circ\text{C}$ ).<sup>28</sup> About 40% quenching was observed during the initial 5 min for DNT, whereas only 15% quenching was observed for TNT during the same time. Plots of fluorescence quenching vs time showed a steep increase in the initial time scale (insets of Figure 2E,F) corresponding to the quenching of superficial layers of the polymer film which quickly come in contact with the analytes on exposure. The subsequent quenching process is controlled by diffusion of the explosives vapors inside the film. Because of high vapor pressure, DNT diffuses easily to the inner layers of polymer and quenches its fluorescence by more than 75% with time. On the other hand, TNT vapors quenches only 54% of the polymer fluorescence on prolonged exposure.

**3.3. Distinction of DNT and TNT Using the Time-Resolved Microwave Conductivity Technique.** The charge carrier generation and its mobility on photoexcitation due to the donor (polymer) and acceptor (DNT and TNT) interactions were studied in the film state using flash-photolysis time-resolved microwave conductivity (FP-TRMC) technique with a 355 nm laser excitation source. This electrode-less technique gives information about the short-range (nanometer scale) intrinsic charge carrier transport properties and could be used to quantify the photoconductivity in terms of  $\phi \sum \mu$ ,<sup>24,29,30</sup> where  $\phi$  is the charge carrier generation quantum yield on excitation with laser light and  $\sum \mu$  is the sum of charge carrier mobilities, i.e., the sum of electron and hole mobilities ( $\mu_e$  and  $\mu_h$ , respectively). Since the extinction coefficients of DNT and TNT (284 and  $44 \text{ M}^{-1} \text{ cm}^{-1}$ , respectively) are about 2–3 orders less than CPDT-BT ( $13\,400 \text{ M}^{-1} \text{ cm}^{-1}$ ) at 355 nm, the possibility for direct excitation of the former would be negligible. No measurable transient signal was obtained for CPDT-BT alone on excitation, indicating that the  $\phi$  is lower than the sensitivity limit. Interestingly, strong transient signals appeared in the presence of DNT, demonstrating the “turn ON” state of photoconductivity (Figure 3A).  $\phi \sum \mu$  values were found to be increased and reaching a maximum of  $1.42 \times 10^{-4} \text{ cm}^2 \text{ V}^{-1} \text{ s}^{-1}$  with increasing DNT concentrations from  $7 \times 10^{-3}$  to  $1.9 \times 10^{-2} \text{ M}$  (11.2–23.7 wt % of DNT in the polymer/DNT mixture). After that,  $\phi \sum \mu$  decreases with further increase in concentration of DNT (Figure S2). The values of  $\phi \sum \mu_{\max}$

and the half-lifetimes of the charge carriers ( $\tau_{1/2}$ ) at different concentrations of DNT are summarized in Figure 3B and in Table 1. The  $\tau_{1/2}$  exhibited an exceptionally long value of 160

**Table 1.**  $\phi \sum \mu_{\max}$  and  $\tau_{1/2}$  in the CPDT-BT/DNT System with Increasing Concentrations of DNT

| [DNT] (mM) | [DNT] (wt %) | $\phi \sum \mu_{\max} (10^{-4} \text{ cm}^2 / (\text{V s}))$ | $\tau_{1/2} (\mu\text{s})$ |
|------------|--------------|--|----------------------------|
| 0          | 0            | <0.1   |                            |
| 7.7        | 11.2         | 0.56   | 160                        |
| 8.8        | 12.6         | 0.94   | 127                        |
| 14         | 18.6         | 1.12   | 20                         |
| 19         | 23.7         | 1.42   | 7.8                        |
| 22         | 26.4         | 0.59   | 4.7                        |
| 26         | 29.8         | 0.59   | 7.0                        |

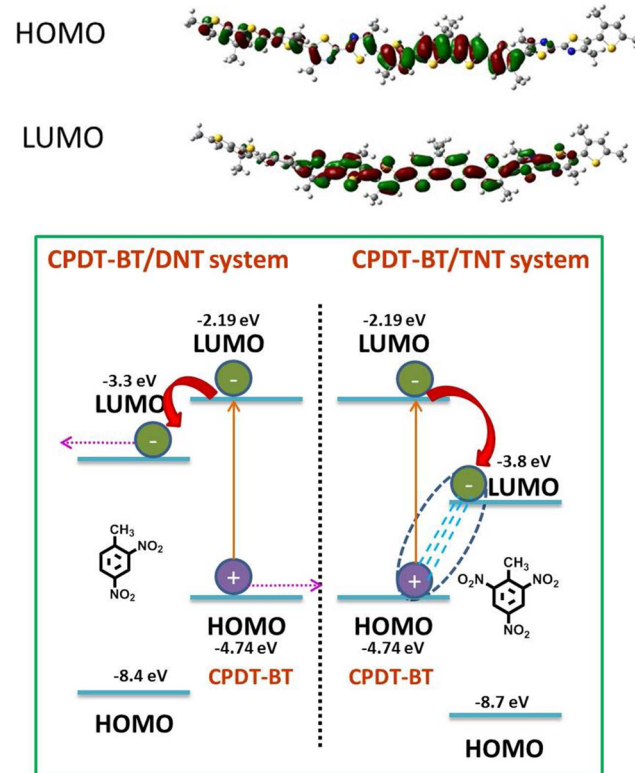
$\mu\text{s}$  when the DNT concentration was 7.7 mM. With increase in the concentration, substantial decrease in the  $\tau_{1/2}$  was observed. It could be assumed that efficient charge carrier (electron and hole) generation was initiated on excitation of the polymer in the presence of DNT. The holes move through the HOMO of the polymer chains by hopping, whereas the electrons would be localized on the DNT molecules. Since the DNT concentration is very low initially, the electrons may not be able to move from one DNT to another. This phenomenon results in a significant reduction in the bulk charge recombination, which allows the hole to travel a long distance without decay and hence the observation of a very long lifetime ( $160 \mu\text{s}$ ). On further addition of DNT, the possibility for the generation of more charge carriers enhances. Similarly, the increase in the number of DNT molecules in the mixture facilitates the electron motion through hopping between neighboring DNT molecules. Because of the combination of these two effects,  $\phi \sum \mu$  increases and reaches the maximum in the presence of 23.7 wt % of DNT. However, because of the electron motion, the possibility for charge recombination also increases at higher concentration of DNT, resulting in the decrease of the charge carrier lifetime ( $7.8 \mu\text{s}$  in the presence of 23.7 wt % of DNT). On further increase of the DNT concentration, the photoabsorption of the polymer decreases, resulting in the lowering of charge carrier generation and hence the  $\phi \sum \mu$  values. Since the recombination rates are sensitive to the density of charges, excitation light intensity dependence of the TRMC signal at lower and higher [DNT] were carried out. In both cases, marginal decrease in the signal intensity and lifetime were observed when the laser intensity was increased from  $4.6 \times 10^{15}$

to  $1.8 \times 10^{16}$  photons cm $^{-2}$  (Figure S3). This could be attributed to the increase in charge recombination rate at higher laser intensity due to the increase in the number of charge carriers. The small dependence on the laser intensity can be rationalized by trap-assisted first-order recombination as has been observed in polymer:fullerene bulk heterojunction films<sup>31</sup> and/or just a trapping process.<sup>29</sup> Surprisingly, no photoconductivity signals were obtained with TNT at any concentrations, even though fluorescence quenching was observed in its presence. The absence of photoconductivity transients gives us an indication that although electron transfer from the polymer occurs in the presence with TNT, charge carriers were not generated.

It can be noted that at lower DNT concentration the TRMC signal shows a rise in the initial time scale before decay, whereas only fast decay was observed at a higher DNT concentration. To understand the origin of such differences in the TRMC signal, detailed transient absorption spectroscopy (TAS) studies were carried out in chlorobenzene. Upon photoexcitation of the polymer using a 355 nm laser source, the triplet state of the polymer with an absorption maximum around 760 nm and a lifetime of 7.8  $\mu$ s was observed (Figure S4). On addition of DNT, the triplet state undergoes quenching, and the lifetime becomes 1.6  $\mu$ s (Figure S4). On the basis of this experiment, it could be assumed that electron transfer could occur from both singlet and triplet excited states of the polymer. Since the triplet formation and the subsequent electron transfer and charge separation take more time when compared to that from the singlet state, maximum population of the charge carriers is observed with a time delay after the photoexcitation. This results in the observation of a rise at the initial time scale of the TRMC signal at low DNT concentration, and the time scale of growth component of the TRMC transient ( $\sim 4 \mu$ s) matches well with the triplet lifetime. At higher DNT concentration, due to the high proximity of DNT molecules around the polymer, electron transfer exclusively happens from the singlet before the generation of triplet states. As a result, rise component was absent when the amount of DNT is higher. TNT can also cause the triplet quenching although the quenching rate was lower ( $3.18 \times 10^5 \text{ s}^{-1}$ ) when compared to that of DNT ( $6.25 \times 10^5 \text{ s}^{-1}$ ). The triplet quenching rate constants and lifetimes obtained from the TAS experiments are given in Table S1.

In order to get an insight into the mechanism of how the photoconductivity is turned “ON” with DNT and remained “OFF” with TNT (though fluorescence has quenched), HOMO–LUMO energy levels of the polymer and the analytes were calculated using density-functional theory (DFT) at the B3LYP/6-31G(d,p) level and are shown in Scheme 3. The HOMO and LUMO levels of CPDT-BT were found to be at -4.74 and -2.19 eV, respectively. The HOMO and LUMO levels of DNT (-8.4 and -3.3 eV, respectively) and TNT (-8.7 and -3.8 eV) were also calculated under similar conditions. The higher HOMO and LUMO energy levels of CPDT-BT when compared to that of both DNT and TNT indicate that fluorescence quenching of the former is due to photoinduced electron transfer to the latter (quencher) molecules. The driving force for the photoinduced electron transfer between polymer and the quenchers was 1.1 and 1.6 eV for DNT and TNT, respectively. It is well-known that the electron and hole pair will exhibit significant Coulombic attraction, despite being located on different entities. The Coulombically bound electron–hole pairs are comprised of

**Scheme 3. HOMO and LUMO Distributions of Energy-Minimized Structures of Two Repeating Units of CPDT-BT (Alkyl Chains Were Replaced by Methyl for Simplicity) Obtained by the DFT Calculation and Schematic Representation of Mechanism of the Distinction of DNT and TNT Using the FP-TRMC Method**



partially separated charges, where the hole is primarily localized on the donor HOMO orbitals and electron is localized on the acceptor LUMO orbitals. Such states can be generally named as “charge transfer (CT) excitons”, and the magnitude of this Coulombic interaction can be termed as “CT state binding energy”.<sup>32</sup> The matching of orbital energy and exchange between the HOMO of the donor and LUMO of the acceptor is an important factor which decides the strength of the exciton formed following the charge transfer between the donor (polymer) and acceptors (explosives analytes). Examination of the energy levels of CPDT-BT, DNT, and TNT (Scheme 3) showed that the LUMO of TNT and HOMO of CPDT-BT are much closer (0.9 eV) than that of the DNT/CPDT-BT complex (1.4 eV). In the former case, there must be a strong overlap between the HOMO of the donor and LUMO of the acceptor which effectively increases the binding energy of the excitons, preventing its dissociation into free charge carriers. On the other hand, in the case of DNT/CPDT-BT complex, the HOMO–LUMO interaction may not be so strong, which allows the splitting of the excitons and generation of free charge carriers resulting in photoconductivity. The mechanism of the distinction of DNT and TNT using the FP-TRMC method could be schematically represented as shown in Scheme 3.

In order to check whether DNT or TNT can be distinguished by employing conventional polymers using TRMC technique, photoconductivity of regioregular poly(3-hexylthiophene): P3HT was studied in the presence of DNT and TNT under similar conditions used for the above

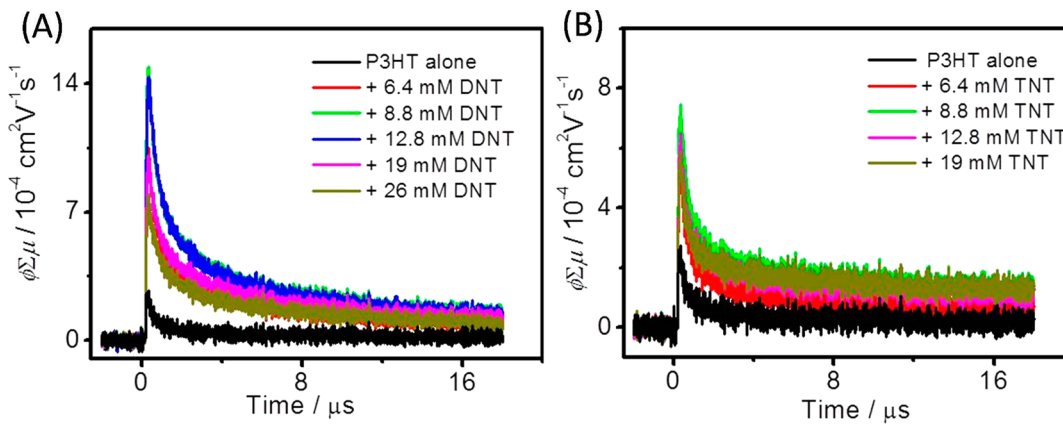


**Figure 4.** FP-TRMC transients of P3HT in presence of increasing concentrations of (A) DNT and (B) TNT.

experiments. P3HT alone exhibited a good photoconductivity transient ( $\phi \sum \mu = 2.7 \times 10^{-4} \text{ cm}^2 \text{ V}^{-1} \text{ s}^{-1}$ ) due to its intrinsic conductivity properties. On addition of both DNT and TNT, the  $\phi \sum \mu$  values were found to increase due to the increase in charge carrier generation. However, the increase in the  $\phi \sum \mu$  values with TNT ( $7.5 \times 10^{-4} \text{ cm}^2 \text{ V}^{-1} \text{ s}^{-1}$ ) was about one-half that of DNT ( $15 \times 10^{-4} \text{ cm}^2 \text{ V}^{-1} \text{ s}^{-1}$ ) (Figure 4). Interestingly, the decay rates of the transients at all concentrations of DNT and TNT were almost similar on the order of about  $0.6 \mu\text{s}$  (Table S2). As evident from Figure 4, the  $\phi \sum \mu$  values of P3HT even in the presence of low amount of DNT or TNT is 1 order higher than that of the CPDT-BT polymer. This could be attributed to the intrinsic high mobility in the crystalline domains of P3HT.<sup>33</sup> Because of its high mobility, the holes may find electrons more easily in the case of P3HT resulting in a faster decay. Thus, the varying concentration of DNT or TNT cannot be uniquely determined from the lifetime and  $\phi \sum \mu$  values of the transients, since it exhibited similar lifetime values at a lower and higher concentration of DNT and TNT. More importantly, DNT and TNT cannot be distinguished using this polymer. In this way CPDT-BT has advantages over the conventional polymers since it does not exhibit any photoconductivity of its own and the concentration of DNT can be estimated from the  $\phi \sum \mu$  and lifetime of the transient species obtained.

#### 4. CONCLUSIONS

In summary, we have introduced a novel method of time-resolved microwave conductivity for the distinction of DNT and TNT which is otherwise challenging with conventional methods. The difference in the HOMO–LUMO energy levels of DNT and TNT was exploited for this purpose in combination with a fluorescent conjugated polymer. The use of the TRMC method in combination with conducting conjugated polymers could be applicable for other explosives derivatives and environmentally important analytes. Since this method is not only sensitive to electron affinities but also to the HOMO–LUMO energy levels of the polymer as well as analytes, it could be able to detect and distinct analytes with comparable electron affinities, which is difficult by conventional methods. When this method is used as a complementary technique to the existing methods, it may provide more reliability and precision to the latter. Design of better polymers may help the detection and distinction processes more efficient and sensitive. The polymer has to satisfy several criteria such as amorphous nature (it enhances the permeability of the analyte

into the polymer layers), high intrapolymer hole mobility to give high TRMC signal, low photo charge carrier generation in the absence of analyte to ensure high contrast of the signal, good binding strength with analyte (which depends on various groups attached to the polymer backbone), and suitable HOMO–LUMO energy levels.

#### ■ ASSOCIATED CONTENT

##### ● Supporting Information

Details of X-ray diffraction pattern of CPDT-BT in thin film state, decrease of FP-TRMC transient intensity of CPDT-BT in the presence of much higher concentrations of DNT, transient absorption experiments of CPDT-BT in the presence of DNT and TNT, table showing decay rates and lifetimes of the transient at 760 nm, laser excitation intensity dependence of the TRMC transients of CPDT-BT in the presence of lower and higher concentrations of DNT, table showing the  $\phi \sum \mu_{\max}$  and  $\tau_{1/2}$  values in P3HT/DNT and P3HT/TNT with increasing concentrations of the analytes. This material is available free of charge via the Internet at <http://pubs.acs.org>.

#### ■ AUTHOR INFORMATION

##### Corresponding Author

\*E-mail saeki@chem.eng.osaka-u.ac.jp (A.S.), seki@chem.eng.osaka-u.ac.jp (S.S.); Fax +81-6-6879-4586; Tel +81-6-6879-4587.

##### Notes

The authors declare no competing financial interest.

#### ■ ACKNOWLEDGMENTS

This work was supported by JSPS Funding Program for Next-Generation World-Leading Researches (NEXT Program), PRESTO-JST, and KAKENHI from the MEXT Japan.

#### ■ REFERENCES

- (1) Toal, S. J.; Sanchez, J. C.; Dugan, R. E.; Trogler, W. C. *J. Forensic Sci.* **2007**, *52*, 79–83.
- (2) Habib, M. K. *Biosens. Bioelectron.* **2007**, *23*, 1–18.
- (3) Rose, A.; Zhu, Z.; Madigan, C. F.; Swager, T. M.; Bulović, V. *Nature* **2005**, *434*, 876–879.
- (4) Riskin, M.; Tel-Vered, R.; Bourenko, T.; Granot, E.; Willner, I. *J. Am. Chem. Soc.* **2008**, *130*, 9726–9733.
- (5) Windsor, E.; Najarro, M.; Bloom, A.; Benner, B., Jr.; Fletcher, R.; Lareau, R.; Gillen, G. *Anal. Chem.* **2010**, *82*, 8519–8524.
- (6) Rao, G. N.; Karpf, A. *Appl. Opt.* **2011**, *50*, A100–A115.

- (7) Zhang, K.; Zhou, H.; Mei, Q.; Wang, S.; Guan, G.; Liu, R.; Zhang, J.; Zhang, Z. *J. Am. Chem. Soc.* **2011**, *133*, 8424–8427.
- (8) Mäkinen, M.; Nousiainen, M.; Sillanpää, M. *Mass Spectrom. Rev.* **2011**, *30*, 940–973.
- (9) Caygill, J. S.; Davis, F.; Higson, S. P. J. *Talanta* **2012**, *88*, 14–29.
- (10) Thomas, S. W., III; Joly, G. D.; Swager, T. M. *Chem. Rev.* **2007**, *107*, 1339–1386.
- (11) Toal, S. J.; Trogler, W. C. *J. Mater. Chem.* **2006**, *16*, 2871–2883.
- (12) Sanchez, J. C.; Trogler, W. C. *J. Mater. Chem.* **2008**, *18*, 3143–3156.
- (13) Nagarjuna, G.; Kumar, A.; Kokil, A.; Jadhav, K. G.; Yurt, S.; Kumar, J.; Venkataraman, D. *J. Mater. Chem.* **2011**, *21*, 16597–16602.
- (14) Sanchez, J. C.; DiPasquale, A. G.; Rheingold, A. L.; Trogler, W. C. *Chem. Mater.* **2007**, *19*, 6459–6470.
- (15) Sohn, H.; Sailor, M. J.; Magde, D.; Trogler, W. C. *J. Am. Chem. Soc.* **2003**, *125*, 3821–3830.
- (16) He, G.; Yan, N.; Yang, J.; Wang, H.; Ding, L.; Yin, S.; Fang, Y. *Macromolecules* **2011**, *44*, 4759–4766.
- (17) Xu, B.; Wu, X.; Li, H.; Tong, H.; Wang, L. *Macromolecules* **2011**, *44*, 5089–5092.
- (18) Nguyen, H. H.; Li, X.; Wang, N.; Wang, Z. Y.; Ma, J.; Bock, W. J.; Ma, D. *Macromolecules* **2009**, *42*, 921–926.
- (19) Qin, A.; Lam, J. W. Y.; Tang, L.; Jim, C. K. W.; Zhao, H.; Sun, J.; Tang, B. Z. *Macromolecules* **2009**, *42*, 1421–1424.
- (20) Chang, C.-P.; Chao, C.-Y.; Huang, J. H.; Li, A.-K.; Hsu, C.-S.; Lin, M.-S.; Hsieh, B. R.; Su, A.-C. *Synth. Met.* **2004**, *144*, 297–301.
- (21) McQuade, D. T.; Pullen, A. E.; Swager, T. M. *Chem. Rev.* **2000**, *100*, 2537–2574.
- (22) Yang, J.-S.; Swager, T. M. *J. Am. Chem. Soc.* **1998**, *120*, 11864.
- (23) Li, K.-C.; Huang, J.-H.; Hsu, Y.-C.; Huang, P.-J.; Chu, C.-W.; Lin, J.-T.; Ho, K.-C.; Wei, K.-H.; Lin, H.-C. *Macromolecules* **2009**, *42*, 3681–3693.
- (24) Balan, B.; Vijayakumar, C.; Saeki, A.; Koizumi, Y.; Seki, S. *Macromolecules* **2012**, *45*, 2709–2719.
- (25) Li, Y. *Acc. Chem. Res.* **2012**, *45*, 723–733.
- (26) Osaka, I.; Shimawaki, M.; Mori, H.; Doi, I.; Miyazaki, E.; Koganezawa, T.; Takimiya, K. *J. Am. Chem. Soc.* **2012**, *134*, 3498–3507.
- (27) Chen, T.-A.; Wu, X.; Rieke, R. D. *J. Am. Chem. Soc.* **1995**, *117*, 233–244.
- (28) Clavaguera, S.; Dautel, O. J.; Hairault, L.; Méthivier, C.; Montméat, P.; Pasquinet, E.; Pradier, C.-M.; Serein-Spirau, F.; Wakim, S.; Veignal, F.; Moreau, J. J. E.; Lére-Porte, J.-P. *J. Polym. Sci., Part A: Polym. Chem.* **2009**, *47*, 4141–4149.
- (29) Saeki, A.; Fukumatsu, T.; Seki, S. *Macromolecules* **2011**, *44*, 3416–3424.
- (30) Saeki, A.; Tsuji, M.; Seki, S. *Adv. Energy Mater.* **2011**, *1*, 661–669.
- (31) Leong, W. L.; Cowan, S. R.; Heeger, A. J. *Adv. Energy Mater.* **2011**, *1*, 517–522.
- (32) Clarke, T. M.; Durrant, J. R. *Chem. Rev.* **2010**, *110*, 6736–6767.
- (33) Bao, Z.; Dodabalapur, A.; Lovinger, A. J. *Appl. Phys. Lett.* **1996**, *69*, 4108–4110.